ISSN 1070-3284, Russian Journal of Coordination Chemistry, 2013, Vol. 39, No. 9, pp. 641–649. © Pleiades Publishing, Ltd., 2013.

Hydrothermal Synthesis, Crystal Structure of Three Novel Complexes Based on Thiabendazole and 1,4-Benzenedicarboxylate Ligands[1]

S. Q. Wei[a, b], C. W. Lin[a], X. H. Yin[b, *], Y. J. Du[b], and Z. Y. Xiong[b]

[a] *College of Chemistry and Chemical Engineering, Guangxi University for Nationalities, Nanning, 530004 P.R. China*
[b] *College of Chemistry and Chemical Engineering, Guangxi University, Nanning, 530006 P.R. China*
**e-mail: yxhphd@163.com*

Received March 22, 2012

Abstract—Three novel metal-organic complexes $[Co(BDC)(TBZ)_2]$ (**I**), $[Cd_2(BDC)_2(TBZ)_2(H_2O)_2] \cdot 2(H_2O)$ (**II**), $[Mn_2(BDC)(TBZ)_4(SO_4)]$ (**III**) (BDC = 1,4-benzenedicarboxylate, TBZ = thiabendazole) have been prepared and characterized by IR spectrum, elemental analysis, thermogravimetric analysis, and single-crystal X-ray diffraction. X-ray structure analysis reveals that both three complexes are one-dimensional chain polymers. The 1D chain architecture of **I** is constructed from terephthalic acid and cobalt atoms. A simultaneous presence of chelating and monodentate coordination modes of BDC ligands is observed in complex **II**. In complex **III**, the coordinated BDC ligands adopt monodentate mode and with SO_4^{2-} anions alternately bridge the Mn^{2+} ions into 1D chains. The 3D structures of the three complexes are stabilized by π–π stacking interactions and hydrogen-bonds.

DOI: 10.1134/S1070328413090091

INTRODUCTION

In the past decades, the design and synthesis of novel organic-inorganic hybrid materials have provoked significant interest owing to their enormous varieties of intriguing structural topologies and their fascinating properties [1–10]. In this process, judicious selection of ligands as basic building blocks is of great importance because slight structural changes about organic building blocks, such as length, flexibility and symmetry, can dramatically change the structural motifs of coordination polymers. As bridging ligands, carboxylates, especially multi-carboxylates, are of immense interest in the construction of polymeric coordination architectures because not only the fact that these polymers have a wide range of structural diversities and potential applications as porous materials and magnetic materials, but also the multi-carboxylates are capable of functioning as hydrogen bond donors and/or acceptors [11]. The auxiliary ligands containing N-donor, such as TBZ, were introduced into the reaction systems so as to inhibit the expansion of polymeric frameworks to obtain the desired low dimensional coordination polymers [12]. TBZ aroused considerable interest in biology and medicine due to its antiproliferative activities [13, 14]. It is an antimicrobial drug belonging to the benzimidazole derivative and has exhibited wide applications in human and veterinary medicine [15]. The employment of mixed ligands has been demonstrated to be a very effective approach for constructing diverse coordination frameworks [16, 17]. However, the hybrid coordination polymers constructed by TBZ and aryl-acid combined are rarely reported [18, 19], although these two ligands are familiar to us. Herein, we report synthesis, crystal structures, elemental analyses, IR spectrum and thermal properties of three novel cobalt(II) complexes with 1,4-benzenedicarboxylate (**BDC**) and thiabendazole (**TBZ**) ligands, $[Co(BDC)(TBZ)_2]$ (**I**), $[Cd_2(BDC)_2(TBZ)_2(H_2O)_2] \cdot 2(H_2O)$ (**II**), $[Mn_2(BDC)(TBZ)_4(SO_4)]$ (**III**), which are formed by π–π stacking interactions and hydrogen bonds.

EXPERIMENTAL

Materials and instrumentation. All chemicals were commercial materials of analytical grade and used without purification. Elemental analysis for C, H, N, and S was carried out on a PerkinElmer 2400 II elemental analyzer. The FT-IR spectrum was obtained on a PE Spectrum One FT-IR Spectrometer Fourier transform infrared spectroscopy in the 4000–400 cm^{-1} regions, using KBr pellets. PerkinElmer Diamond TG/DTA thermal analyzer was used to record simultaneous TG and DTG curves in the static air atmosphere at a heating rate of 10 K min^{-1} in the temperature range 25–1000°C using platinum crucibles.

Synthesis of I. A solution of TBZ (0.201 g, 1 mmol) in 3 mL DMF was added dropwise with stirring at room temperature to a solution of $Co(NO_3)_2 \cdot 6H_2O$

---

[1] The article is published in the original.

(0.291 g, 1 mmol), H_2BDC (0.1660 g, 1 mmol) in the mixture of 10 mL water and 5 mL ethanol. Then an aqueous solution of sodium hydroxide was added dropwise with stirring to adjust the pH value of the solution being 6. The resulting mixture was sealed in a 23 mL Teflon-lined stainless reactor, kept under autogenous pressure at 130°C for 72 h, and then slowly cooled to room temperature at a rate of 5°C per hour. The red block crystals suitable for X-ray diffraction were isolated directly, washed with ethanol and dried in air (the yield was 65% based on Co).

For $C_{28}H_{18}N_6O_4S_2Co$
anal. calcd., %: C, 53.76; H, 2.90; N, 13.43; S, 10.25.
Found, %: C, 53.78; H, 2.93; N, 13.41; S, 10.24.

IR data (KBr; ν, cm^{-1}): 3490 br, 1653 s, 1593 v.s, 1553 s, 1495 m, 1218 m, 1116 m, 860 m, 720 s, 647 w.

Synthesis of II. TBZ (0.201 g, 1 mmol) and H_2BDC (0.1660 g, 1 mmol) were dissolved in the mixture of 6 mL H_2O and 5 mL DMF. Then an aqueous solution of sodium hydroxide was added dropwise with srirring to adjust the pH value of the solution being 6. At last, 10 mL aqueous solution of $Cd(NO_3)_2 \cdot 4H_2O$ (0.3085 g, 1 mmol) was input. The resulting mixture was sealed in a 23 mL Teflon-lined stainless reactor, kept under autogenous pressure at 130°C for 72 h, and then slowly cooled to room temperature at a rate of 5°C per hour. The red block crystals suitable for X-ray diffraction were isolated directly, washed with ethanol and dried in air (the yield was 45% based on Cd).

For $C_{36}H_{30}N_6O_{12}S_2Cd_2$
anal. calcd., %: C, 42.08; H, 2.94; N, 8.18; S, 6.24.
Found, %: C, 42.09; H, 2.96; N, 8.17; S, 6.25.

IR data (KBr; ν, cm^{-1}): 3410 br, 1649 s, 1596 v.s, 1556 s, 1494 s, 1221 m, 1096 m, 850 m, 709 m.

Synthesis of III. The same synthetic procedure as that for **I** was used except that $Co(NO_3)_2 \cdot 6H_2O$ (0.291 g, 1 mmol) was replaced by $MnSO_4 \cdot H_2O$ (0.169 g, 1 mmol). The red block crystals of **III** were obtained in 55% yield based on Mn.

For $C_{48}H_{32}Mn_2N_{12}O_8S_5$
anal. calcd., %: C, 49.06; H, 2.74; N, 14.30; S, 13.64.
Found, %: C, 49.05; H, 2.77; N, 14.28; S, 13.62.

IR data (KBr; ν, cm^{-1}): 3420 br, 1645s, 1595 v.s, 1555 s, 1498 s, 1235 m, 1104 m, 1092 m, 845 m, 713 s, 644 m.

X-ray structure determination. Single crystal of the complex was mounted on glass fiber and measured on a Bruker SMART CCD area detector at 296 K using graphite monochromated MoK_α radiation ($\lambda = 0.71073$ Å). Empirical absorption corrections were applied using the SADABS program [20]. The structure was solved by the direct method and refined by full-matrix least squares on F^2 using the SHELXTL program [21]. All non-hydrogen atoms were refined anisotropically. Hydrogen atoms were set in calculated positions and refined by a riding mode, with a common thermal parameter. The crystal data and structure refinement details for three complexes are shown in Table 1. Selected bond lengths and angles of the complexes are listed in Table 2, and possible hydrogen bond geometries are given in Table 3.

Supplementary material has been deposited with the Cambridge Crystallographic Data Centre (nos. 869946 (**I**), 869945 (**II**), 869947 (**III**); deposit@ccdc.cam.ac.uk or http://www.ccdc.cam.ac.uk).

RESULTS AND DISCUSSION

The structure of the compound **I** is formed by infinite one-dimensional chains. The simplest coordination pattern is observed in compound **I**, where each cobalt atom has an octahedral environment formed by four nitrogen atoms (N(1), N(2), N(3), N(4)) from two chelated TBZ ligands and two O atoms (O(1), O(3)) from different BDC ligands (Fig. 1). The carboxy groups of BDC ligands are coordinated in a monodentate mode. In the overall structure of **I**, units of $[Co(TBZ)]^{2+}$ are connected by the bridging BDC ligands to generate a zigzag chain (Fig. 2). The 1D chains are linked by weak N(3)–H(3*A*)···O(2)$^{\#}$ (symmetry code: $^{\#}\,x + 1/2, y - 1/2, z + 3/2$) hydrogen bonds (Table 3) with the distance of 2.669(2) Å to yield a layered network. Figure 2 also reveals that π–π interactions exist between TBZ ligands with the centroid-centroid distances of 3.767 Å. Such contacts link the 2D layers into a 3D structure.

As shown in Fig. 3 for compound **II**, the BDC ligands have two types: A is bidentate and B is monodentate. The two crystallographically independent Cd atoms (Cd(1) and Cd(2)) are bridged by one BDC ligand which acts as a long bridge through the benzene ring. We can find that there are two independent Cd(II) centers showing two different coordination environments. The Cd(1) ion is seven-coordinated with four O atoms (O(6), O(7), O(8), O(9)) from two chelated BDC ligands, a water molecule (O(12)), and two nitrogen atoms (N(4), N(6)) from chelated TBZ to form a distorted decahedron as shown in Fig. 4. The Cd(2) center is coordinated to two N donors (N(1), N(3)) of one TBZ, three oxygen atoms (O(2), O(4), O(5)) belonging to two different carboxyl groups of two different terephthalic acid molecules and one water molecule (O(1)), forming a distorted octahedral geometry. The structure of **II** is stabilized by hydrogen bonds formed by N–H···O hydrogen bonds from N–H of TBZ together with water molecule (N(2)–H(2)···O(10), N(5)–H(5)···O(11)) and by the water molecule with oxygen atoms of BDC ligands (Table 3). The crystal structure of compound **II** is also stabilized

Table 1. Crystallographic data and details of structure refinements for complexes **I–III**

Parameter	Value		
	I	**II**	**III**
Formula weight	625.53	1027.58	1175.04
Crystal system	Orthorhombic	Triclinic	Triclinic
Space group	*Pbcn*	$P\bar{1}$	$P\bar{1}$
a, Å	12.778(4)	11.031(3)	11.175(2)
b, Å	10.465(3)	11.425(4)	13.791(3)
c, Å	20.000(5)	16.625(4)	16.842(3)
α, deg	90	94.330(3)	92.520(3)
β, deg	90	94.600(3)	95.221(3)
γ, deg	90	113.926(3)	111.443(3)
Volume, Å^3	2674.6(13)	1895.5(10)	2397.6(8)
Z	4	2	2
ρ_{calcd}, g cm^{-3}	1.553	1.800	1.628
Absorption coefficient, mm^{-1}	0.846	1.305	0.815
F(000)	1276	1024	1196
Crystal size, mm	0.22 × 0.18 × 0.15	0.28 × 0.22 × 0.17	0.22 × 0.18 × 0.15
θ Range for data collection, deg	2.04–25.10	1.24–25.10	1.22–25.10
Reflections collected	13693	10383	13265
Independent reflections (R_{int})	2381 (0.0254)	6648 (0.0197)	8448 (0.0232)
Reflections with $I > 2\sigma(I)$	2016	5700	5956
Completeness to θ = 25.00, %	100.0	98.5	98.8
Max and min transmission	0.8836 and 0.8358	0.8087 and 0.7115	0.8875 and 0.8411
Parameters	186	523	676
Goodness-of-fit on F^2	1.084	1.057	1.023
R indices ($I > 2\sigma(I)$)	$R_1 = 0.0285$, $wR_2 = 0.0789$	$R_1 = 0.0400$, $wR_2 = 0.1304$	$R_1 = 0.0400$, $wR_2 = 0.1085$
R indices (all data)	$R_1 = 0.0353$, $wR_2 = 0.0819$	$R_1 = 0.0459$, $wR_2 = 0.1356$	$R_1 = 0.0627$, $wR_2 = 0.1361$
$\Delta\rho_{max}/\Delta\rho_{min}$, e Å^{-3}	0.281 and –0.264	1.311 and –0.723	0.520 and –0.334

by π–π stacking of the aromatic rings from the TBZ ligands and BDC ligands (Fig. 4). A 3D architecture was constructed by hydrogen bonds and π–π stacking interactions.

A perspective view of the molecular structure of the complex **III** along with the atom-numbering scheme is depicted in Fig. 5. Each Mn(II) center adopts a distorted octahedral coordination environment with one oxygen atom (O(1)) from BDC ligand, one oxygen atom (O(8)) from SO_4^{2-} anion, and four nitrogen atoms (N(7), N(8), N(10), N(12)) from two chelating TBZ ligands. The environment of Mn(1) is modified by incorporation of a coordinating oxygen atom (O(8)) into a *trans* position to one of the nitrogen atoms (N(8)), resulting in change of a coordination mode of BDC ligand from chelating to monodentate. Therefore, the coordinated BDC ligands adopt monodentate mode and with SO_4^{2-} anions alternately bridge the Mn^{2+} ions into 1D chains. As shown in Fig. 6, the adjacent chains are connected through N–H···O hydrogen bonds from N–H of TBZ together with carboxylic O atom of BDC (N(3)–H(3)···O(2), N(5)–H(5)···O(6), N(11)–H(11)···O(8), N(9)–H(9)···O(3)). TBZ ligands locate at both side of the molecule and there are π–π stacking interactions between them of adjacent chains. The π–π stacking and hydrogen bonds interlink the 1D layers to generate 3D supramolecular architectures.

Table 2. The selected bond lengths (Å) and angles (deg) for complex **I–III***

Bond	*d*, Å	Bond	*d*, Å
		I	
Co(1)–O(1*A*)	2.0696(14)	Co(1)–O(1)	2.0696(14)
Co(1)–N(2*A*)	2.1562(16)	Co(1)–N(2)	2.1562(16)
Co(1)–N(1*A*)	2.1856(17)	Co(1)–N(1)	2.1856(17)
		II	
Cd(1)–O(7)	2.305(3)	Cd(1)–N(4)	2.315(3)
Cd(1)–O(8)	2.326(3)	Cd(1)–O(12)	2.331(4)
Cd(1)–N(6)	2.440(4)	Cd(1)–O(9)	2.542(3)
Cd(1)–O(6)	2.543(3)	Cd(2)–O(2)	2.227(3)
Cd(2)–N(1)	2.279(3)	Cd(2)–O(1)	2.295(3)
Cd(2)–O(5)	2.304(4)	Cd(2)–N(3)	2.408(4)
Cd(2)–O(4)	2.489(4)		
		III	
Mn(1)–O(1)	2.098(2)	Mn(1)–O(8)	2.163(2)
Mn(1)–N(8)	2.284(3)	Mn(1)–N(7)	2.286(3)
Mn(1)–N(12)	2.303(3)	Mn(1)–N(10)	2.344(3)
Mn(2)–O(4*A*)	2.121(2)	Mn(2)–O(7)	2.153(2)
Mn(2)–N(1)	2.276(3)	Mn(2)–N(2)	2.303(3)
Mn(2)–N(6)	2.312(3)	Mn(2)–N(4)	2.335(3)
Angle	ω, deg	Angle	ω, deg
		I	
O(1*A*)Co(1)O(1)	95.96(8)	O(1*A*)Co(1)N(2*A*)	162.86(6)
O(1)Co(1)N(2*A*)	91.62(6)	O(1*A*)Co(1)N(2)	91.62(6)
O(1)Co(1)N(2)	162.86(6)	N(2*A*)Co(1)N(2)	85.41(9)
O(1*A*)Co(1)N(1*A*)	101.97(6)	O(1)Co(1)N(1*A*)	86.36(6)
N(2*A*)Co(1)N(1*A*)	93.82(6)	N(2)Co(1)N(1*A*)	77.02(6)
O(1*A*)Co(1)N(1)	86.36(6)	O(1)Co(1)N(1)	101.97(6)
N(2*A*)Co(1)N(1)	77.02(6)	N(2)Co(1)N(1)	132.35
N(1*A*)Co(1)N(1)	167.65(9)		
		II	
O(7)Cd(1)N(4)	91.58(12)	O(7)Cd(1)O(8)	110.37(13)
N(4)Cd(1)O(8)	92.19(12)	O(7)Cd(1)O(12)	147.46(13)
N(4)Cd(1)O(12)	118.92(14)	O(8)Cd(1)O(12)	81.39(13)
O(8)Cd(1)O(9)	53.29(11)	O(12)Cd(1)O(9)	79.71(14)
N(6)Cd(1)O(9)	148.33(13)	O(7)Cd(1)O(6)	53.95(10)
N(4)Cd(1)O(6)	128.60(11)	O(8)Cd(1)O(6)	132.45(11)
O(9)Cd(1)O(6)	79.34(11)	O(2)Cd(2)N(1)	97.58(13)
O(2)Cd(2)O(5)	85.00(14)	N(1)Cd(2)O(5)	113.65(13)
N(1)Cd(2)N(3)	72.47(13)	O(1)Cd(2)N(3)	90.19(13)
O(5)Cd(2)N(3)	100.30(13)	O(2)Cd(2)O(4)	106.02(13)
N(1)Cd(2)O(4)	151.59(12)	O(1)Cd(2)O(4)	94.43(11)
O(5)Cd(2)O(4)	54.45(11)	N(3)Cd(2)O(4)	83.99(13)
		III	
O(1)Mn(1)O(8)	93.59(10)	O(1)Mn(1)N(8)	91.06(10)
O(8)Mn(1)N(8)	175.04(10)	O(1)Mn(1)N(7)	101.85(10)
O(8)Mn(1)N(7)	103.04(10)	N(8)Mn(1)N(7)	74.27(10)
N(8)Mn(1)N(12)	93.26(10)	N(7)Mn(1)N(12)	159.24(10)
N(8)Mn(1)N(10)	91.75(10)	N(7)Mn(1)N(10)	90.28(10)
N(12)Mn(1)N(10)	73.26(9)		

* Symmetry transformations used to generate equivalent atoms: (*A*): $-x + 2, y, -z + 3/2$ (**I**); $x + 1, y, z$ (**III**).

Table 3. Geometric parameters of hydrogen bonds of complexes **I–III**

Contact D–H···A	Distance, Å			Angle DHA, deg	Symmetry codes
	D–H	H···A	D···A		
I					
N(3)–H(3*A*)···O(2)	0.86	1.810	2.669(2)	176	$x + 1/2, y - 1/2, -z + 3/2$
II					
N(2)–H(2)···O(10)	0.86	1.97	2.806(5)	164	$x + 1, y, z$
N(5)–H(5)···O(11)	0.86	1.90	2.760(5)	178	$-x + 1, -y + 1, -z + 2$
O(1)–H(1*D*)···O(6)	0.85	1.82	2.669(5)	173	$x + 1, y, z$
O(1)–H(1*C*)···O(3)	0.85	1.78	2.629(5)	172	
O(10)–H(10*C*)···O(5)	0.85	2.28	3.085(5)	157	$-x + 1, -y, -z + 1$
O(10)–H(10*D*)···O(7)	0.85	2.10	2.903(5)	157	$-x + 1, -y + 1, -z + 1$
O(11)–H(11*D*)···O(8)	0.85	1.91	2.731(5)	163	$x, y - 1, z$
O(11)–H(11*C*)···O(1)	0.85	2.06	2.886(5)	163	$x - 1, y, z$
O(12)–H(11*C*)···O(9)	0.85	2.29	3.134(6)	176	
O(12)–H(11*D*)···O(4)	0.85	1.87	2.716(5)	176	$x - 1, y, z$
III					
N(3)–H(3)···O(2)	0.86	1.87	2.721(4)	172	$x, y - 1, z$
N(5)–H(5)···O(6)	0.86	1.89	2.734(4)	165	$-x + 2, -y + 2, -z + 1$
N(11)–H(11)···O(8)	0.86	2.13	2.912(4)	151	$-x + 2, -y + 2, -z$
N(9)–H(9)···O(3)	0.86	1.89	2.738(4)	169	$x + 1, y + 1, z$

In the IR spectrum of three complexes, the strong and broad absorption bands at about 3460–3120 cm^{-1} are attributed to the symmetric O–H stretching modes and O–H bending modes, respectively. The N–H stretching band at 3093 cm^{-1} has shifted to about 3102 cm^{-1} in three complexes. One of the $\nu(C{=}N)_{iz}$ and $\nu(C{=}N)_{tz}$ bands (1577 and 1480 cm^{-1}, respectively) changes to 1593 and 1495 cm^{-1} in **I**, 1596 and 1494 cm^{-1} in **II**, 1595 and 1498 cm^{-1} in **III**, indicating the TBZ ligand is chelat-

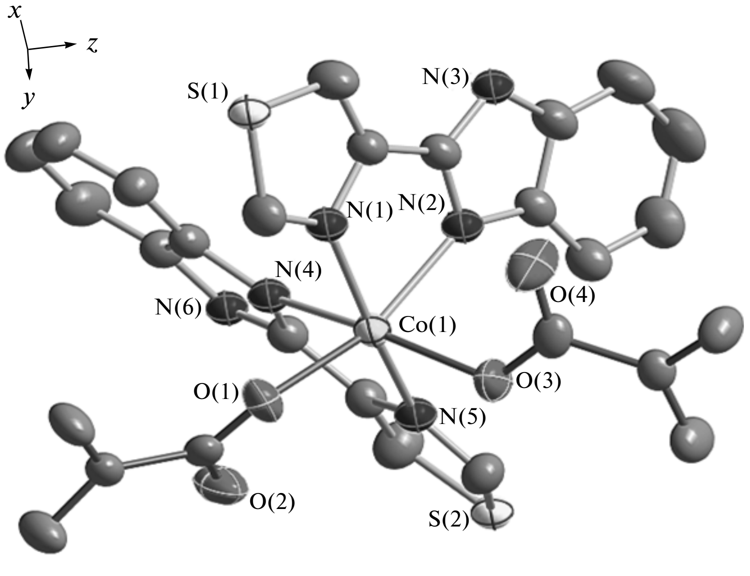

Fig. 1. The coordination environment of Co^{2+} ion of complex **I**. All the hydrogen atoms are omitted for clarity.

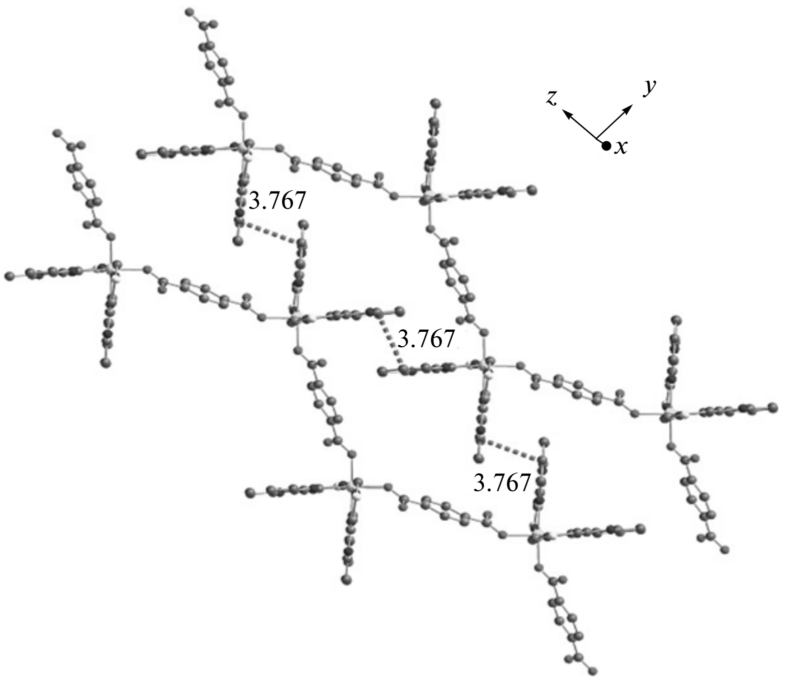

Fig. 2. The 1D chain and the π–π stacking interactions of complex **I**. Unnecessary atoms are omitted for clarity.

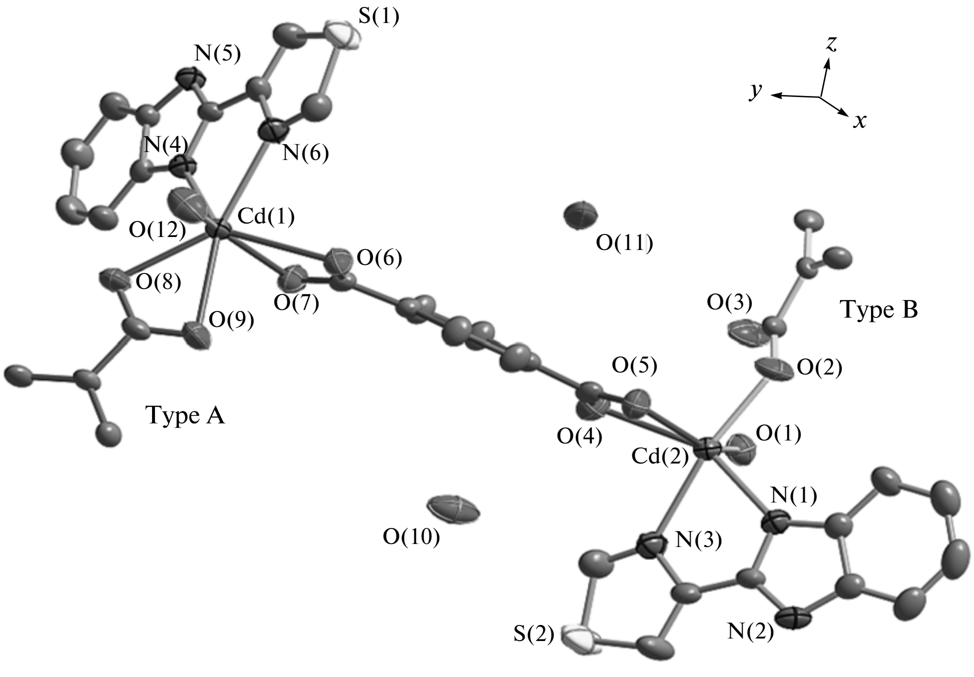

Fig. 3. The coordination environment of Cd^{2+} ion of complex **II**. All the hydrogen atoms are omitted for clarity.

ed through the imidazolic and thiazolic nitrogens. The C–S stretching band (at 1228 cm^{-1} for the free ligand) does not largely change (1218 cm^{-1} in **I**, 1221 cm^{-1} in **II**, and 1235 cm^{-1} in **III**), suggesting the sulphur atom in the thiazole ring is uncoordinated. The COO^- is coordinated with its asymmetric and symmetric stretching appearing at about 1649, 1553 cm^{-1}. The N–H vibrations at about 1096 cm^{-1}

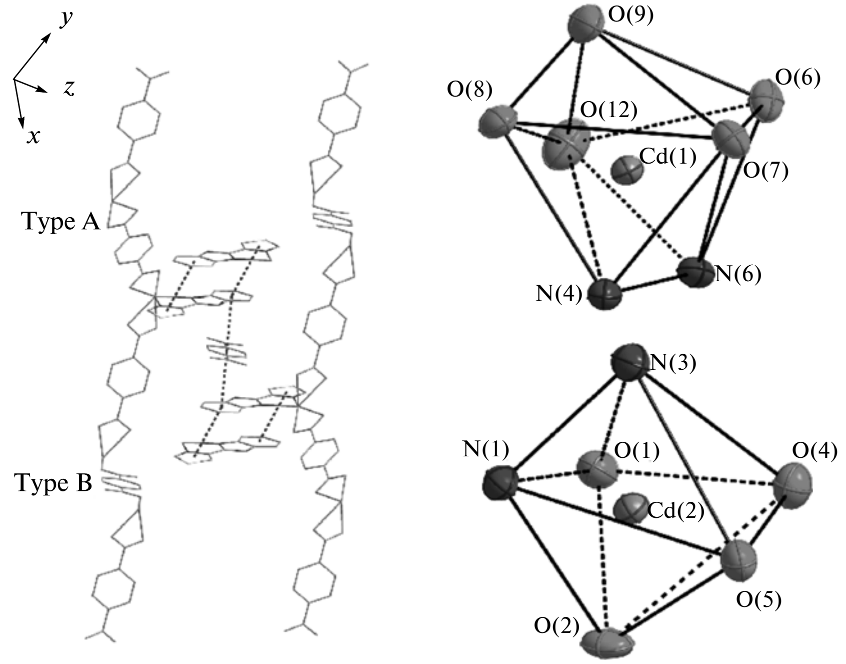

Fig. 4. The 1D chain, the π–π stacking interactions and the coordination polyhedron of the Cd^{2+} ion of complex **II**. Unnecessary atoms are omitted for clarity.

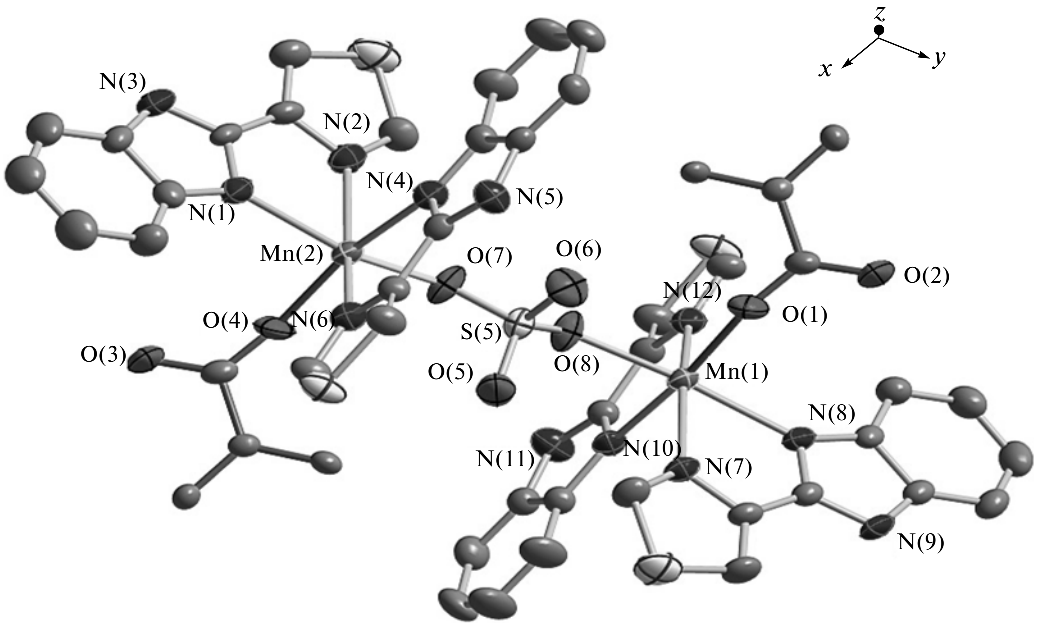

Fig. 5. The coordination environment of Mn^{2+} ion of the complex **III**. All the hydrogen atoms are omitted for clarity.

is observed in all complexes. In complex **III**, SO_4^{2-} anion has a strong absorption in the IR spectrum at 1147 cm^{-1}.

In TG curve of the complex **I**, two weight loss steps exist and the decomposition mainly takes place at 365 and 428°C. The first weight loss stage may be related to the removal of BDC (found: 28.15%, calcd. 26.24%), and the second corresponds to the release of TBZ (found: 61.24%, calcd. 64.32%). Above 835°C, nearly no weight loss is observed.

The thermal decomposition curve of complex **II** exhibits three stages. The complex loses water molecules at 162°C, the weight loss found of 8.5% was con-

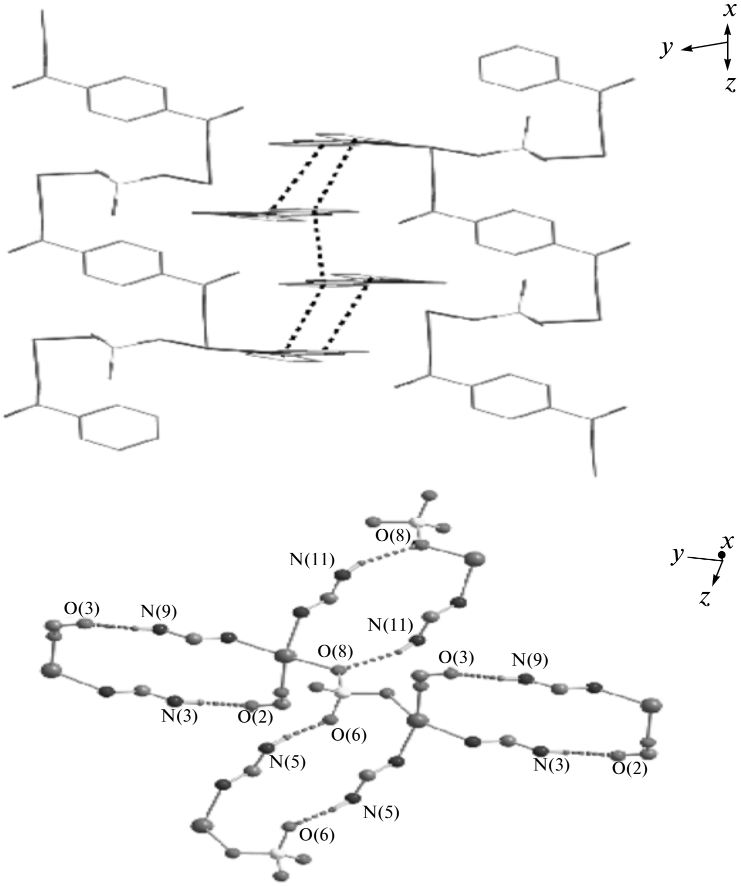

Fig. 6. A perspective view of H-bonding and the π–π stacking interactions of complex **III**. Unnecessary atoms are omitted for clarity.

sistent with that calculated 7.0%. The anhydrous complex loses 32.45% of total weight in the 313–475°C temperature range, corresponding to the removal of two BDC ligands (calcd. 31.94%). When the temperature holds on rising, the products lose 38.7% of the total weight in the temperature range of 480–810°C, which is related to the loss of TBZ (calcd. 39.14%). The residual percentage weight at the end of the decomposition of the complex is observed 25.02%.

TG of complex **III** indicates that three loses 12.58% of total weight from 374 to 430°C, corresponding to the removal of the coordinated BDC (calcd. 8.18%). Upon temperature increase, the TBZ decomposes gradually, a series of complicated and consecutive weight losses occur

ACKNOWLEDGMENTS

The authors thank the National Natural Science Foundation of China (no. 20761002), P.R. China, the Natural Science Foundation of Guangxi (no. 0832080), P.R. China.

REFERENCES

1. Li, J.R., Kuppler, R.J., and Zhou, H.C., *Chem. Soc. Rev.*, 2009, vol. 38, p. 1477.
2. Zheng, S.R., Yang, Q.Y., Yang, R., et al., *Cryst. Growth Des.*, 2009, vol. 9, p. 2341.
3. Janiak, C., *Dalton Trans.*, 2003, p. 2781.
4. Steel, P.J., *Acc. Chem. Res.*, 2005, vol. 38, p. 243.
5. Murray, L.J., Dincă, M., and Long, J.R., *Chem. Soc. Rev.*, 2009, vol. 38. p. 1294.
6. Lin, W.B., Ma, L., and Evans, O.R., *Chem. Commun.*, 2000, p. 2263.
7. Hao Hu-Jun, Lin Cui-Wu, Yin Xian-Hong, and Zhang Feng, *J. Coord. Chem.*, 2011, vol. 64, p. 965.
8. Go Yong Bok, Wang Xiqu, Anokhina, E.K., and Jacobson, A.J., *Inorg. Chem.*, 2005, vol. 44, p. 8265.
9. Ye Bao-Hui, Williams, I.D., Li, and Xiao-Yuan, *J. Inorg. Biochem.*, 2002, vol. 92, p. 128.
10. Pruchnik, F.P., Dawid, U., and Kochel, A., *Polyhedron*, 2006, vol. 25, p. 3647.
11. Ye, B.-H., Tong, M.-L., and Chen, X.-M., *Coord. Chem. Rev.*, 2005, vol. 249, p. 545.
12. Xu Yan-Qing, Zhou You-Fu, Yuan Da-Qing, and Hong Mao-Chun, *Chin. J. Struct. Chem.*, 2006, vol. 25, p. 1161.

13. Devereux, M., McCann, M., Shea, D.O., et al., *Inorg. Biochem.*, 2004, vol. 98, p. 1023.
14. *Human Antiparasitic Drugs: Pharmacology and Usage*, James, D.M. and Gilles, H.M., Eds., New York: John Wiley & Sons, 1996, p. 206.
15. Kaniskan, N. and Ogretir, C., *J. Mol. Struct.*, 2002, vol. 584, p 45.
16. Liu, G.X., Huang, R.Y., Huang, L.F., et al., *CrystEngComm*, 2009, vol. 11, p. 643.
17. Lu, W.G., Jiang, L., and Lu, T.B., *Cryst. Growth Des.*, 2008, vol. 8, p. 986.
18. Wang Jia-Jun, Ming, L.V., Sun Ya-Ming, and Cui Yun-Cheng, *Chin. J. Struct. Chem.*, 2009, vol. 28, p. 34.
19. Wang Jia-Jun, Cui Yun-Cheng, Liu Li-Hui, and Huang Yan-Ju, *Chin. J. Struct. Chem.*, 2010, vol. 29, p. 240.
20. Sheldrick, G.M., *SADABS, Program for Empirical Absorption Correction of Area Detector*, Göttingen (Germany): Univ. of Göttingen, 1996.
21. Sheldrick, G.M., *Acta Crystallogr., A*, 2008, vol. 64, p. 112.